EUROPHYSICS LETTERS 1 February 1995

Europhys. Lett., **29** (4), pp. 345-350 (1995)

Stacks of Fluid Membranes under Pressure and Tension.

R. R. NETZ (*)(§) and R. LIPOWSKY (*)(**)

(*) *Institut für Festkörperforschung, Forschungszentrum Jülich - 52425 Jülich, Germany*
(**) *Max-Planck-Institut für Kolloid- und Grenzflächenforschung Kantstr. 55, 14513 Teltow-Seehof, Germany*

(received 11 August 1994; accepted in final form 19 December 1994)

PACS. 82.70-y - Disperse systems.
PACS. 64.60-i - General studies of phase transitions.
PACS. 05.40+j - Fluctuation phenomena, random processes, and Brownian motion.

Abstract. - Stacks of non-intersecting fluid membranes which are governed by bending rigidity and lateral tension and hold together by an external pressure are studied theoretically using Monte Carlo simulations. Thermal shape fluctuations give rise to an effective repulsion between the individual membranes, which depends sensitively on the relative strength of bending rigidity and lateral tension. For tensionless stacks, the strength of this repulsion is by a factor of two smaller than previously estimated and does not depend on the number of membranes in the stack within the numerical accuracy. For a pair of two membranes, the universal scaling form of this repulsion is determined for varying ratios of the bending rigidity and the surface tension.

The effective or renormalized interaction between bilayer membranes in a lamellar stack or bunch is determined by the interplay between direct molecular forces and fluctuation forces due to thermal excitations [1]. Direct forces for amphiphilic sheets separated by layers of solvent comprise the hard-wall repulsion at zero separation, preventing the membranes from crossing each other, the omnipresent van der Waals attraction, and electrostatic interactions. An external pressure can be applied by various means, including mechanical, osmotic, and vapor-pressure techniques [2], and acts as an additional potential which is linearly proportional to the separation between the membranes. For fluid membranes, the dominant excitations are usually bending modes only. In many experimental situations, however, a lateral tension is present in addition [3].

In this letter, we determine the strength of the effective repulsion V_{Fl} due to shape fluctuations which are controlled by bending rigidity *and* surface tension in the presence of hard-wall interactions only (1). This is achieved by determining the mean separation ℓ between membranes which are bound by an external pressure, from which the fluctuation strength is deduced. For the case of zero lateral tension, the fluctuation potential is given by

$$V_{\mathrm{Fl}}(\ell) \approx c_{\mathrm{Fl}} T^2 / \kappa \ell^2 \tag{1}$$

(§) Present address: Department of Physics FM-15, University of Washington, Seattle WA 98195, USA.

(1) For two interacting membranes, the free energy F per unit area and the mean separation ℓ are related via $\partial F(P)/\partial P = \ell$. Inverting this relation to obtain $P = P(\ell)$, the Legendre-transformed free-energy density (which is the fluctuation potential) is given by $V_{\mathrm{Fl}}(\ell) = F(P(\ell)) - P\ell$, with $-\partial V_{\mathrm{Fl}}(\ell)/\partial \ell = P$.

for large separations ℓ between neighbouring membranes with κ being the bending modulus. Our Monte Carlo (MC) data lead to $c_{\mathrm{Fl}} \simeq 3\pi^2/256$, which is half of one of the estimates due to Helfrich [4]. Numerically, c_{Fl} does not seem to depend on the number of membranes, as explicitly checked for stacks of two to four membranes. Therefore, as far as this fluctuation potential is concerned, stacks of membranes which do not experience short-ranged attractive forces can be regarded as assemblies of independent pairs of membranes. Consequently, the influence of an additional lateral tension is studied below for a *single* pair of membranes, for which we obtain the general form of the fluctuation repulsion. In the limit of small tension, this general form reduces to (1) for small ℓ.

To proceed, consider the effective Hamiltonian for a stack of N membranes under external pressure P, as given by

$$\mathcal{H}\{l_1, \ldots, l_N\} = \int \mathrm{d}^2\boldsymbol{x} \left\{ \sum_{n=1}^{N} \left[\frac{\kappa_n}{2} (\nabla^2 l_n(\boldsymbol{x}))^2 + \frac{\sigma_n}{2} (\nabla l_n(\boldsymbol{x}))^2 \right] + P(l_N(\boldsymbol{x}) - l_1(\boldsymbol{x})) \right\}, \quad (2)$$

where the displacement field $l_n(\boldsymbol{x})$ parametrizes the shape of the n-th membrane. The hard-wall interaction is implicitly embodied by the constraint $l_1 < l_2 < \ldots < l_N$. In all what follows we only consider i) the *symmetric* case with identical bending moduli $\kappa \equiv \kappa_n$ and surface tensions $\sigma \equiv \sigma_n$ for $n = 1, \ldots, N$, and ii) the *asymmetric* case with $\kappa \equiv \kappa_n$ and $\sigma \equiv \sigma_n$ for $n = 2, \ldots, N$ and $\kappa_1 = \sigma_1 = \infty$. In the latter case, the first membrane acts as a flat substrate. After discretization of the coordinate $\boldsymbol{x}$ with lattice constant $a_{\parallel}$ and using the dimensionless continuous height variables $z_n \equiv l_n \sqrt{\kappa/T}/a_{\parallel}$, the resultant parameters are the rescaled pressure $p \equiv P a_{\parallel}^3/\sqrt{\kappa T}$ and the dimensionless crossover parameter $\omega \equiv a_{\parallel}\sqrt{\sigma/\kappa}$. In the MC simulations we typically did 10^7 MC steps using square lattices with up to 12500 sites [5]. Because of the enormous numerical effort, our studies were restricted to $N \leqslant 4$.

We first consider tensionless stacks, for which $\omega = 0$; figure 1*a*) shows the mean separation $\ell \equiv \langle l_2 - l_1 \rangle \sim \langle \delta z \rangle \equiv \langle z_2 - z_1 \rangle$, the roughness $\xi_\perp \equiv (\langle (l_2 - l_1 - \ell)^2 \rangle)^{1/2} \sim \langle \delta z^2 \rangle_{\mathrm{c}}^{1/2} \equiv \equiv (\langle \delta z^2 \rangle - \langle \delta z \rangle^2)^{1/2}$, and the parallel correlation length $\xi_{\parallel} \equiv \exp[2\pi \langle (\nabla \delta z)^2 \rangle]$ [6] for the case of two identical membranes as a function of the pressure p. The data are consistent with the ratio $\ell/\xi_\perp \approx \mathcal{G}_\perp \simeq \sqrt{5}$ [7]. The observed behavior $\sim p^{-1/3}$, as denoted by the straight lines, follows from minimizing the superposition of the pressure interaction and the fluctuation repulsion, $P\ell + V_{\mathrm{Fl}}(\ell)$, leading to $\ell \approx (2c_{\mathrm{Fl}} T^2/\kappa P)^{1/3}$ (see (1)). For the other length scales, one in addition uses the scaling law $\ell \sim \xi_\perp \sim \xi_{\parallel} a_{\parallel} \sqrt{T/\kappa}$. From the fit to the separation ℓ we estimate $c_{\mathrm{Fl}} = 0.116 \pm 0.002$, which is very close to $3\pi^2/256$ and thus exactly half the value proposed originally [4] and deduced experimentally by X-ray scattering on lamellar phases in oil-water-surfactant mixtures, [8] a discrepancy still unresolved (2). The value of c_{Fl} has also been estimated, in the limit of large N, using functional renormalization [9], leading to $c_{\mathrm{Fl}} \simeq 0.0810$.

Another geometry which has been studied by MC simulations are N identical membranes confined between two rigid walls [10, 11]. The separation between these walls was taken to be $(N + 1)\,\ell$ so that the mean separation of all nearest-neighbor surfaces is close to ℓ. The excess free-energy density $V_{\mathrm{Fl}}^{(N)}(\ell)$ per membrane was determined via the internal energy density leading to $c_{\mathrm{Fl}}^{(1)} \simeq 0.080$, $c_{\mathrm{Fl}}^{(3)} \simeq 0.093$, $c_{\mathrm{Fl}}^{(5)} \simeq 0.097$ for $N = 1$, 3 and 5 membranes [10]. Extrapolation to large N gave the estimate $c_{\mathrm{Fl}}^{\infty} \simeq 0.106$ which is somewhat smaller than our value obtained in the pressure ensemble. The latter value should be more reliable, however, since it is independent of N and thus involves no extrapolation procedure.

---

(2) Additional short-ranged interactions do not change the fluctuation amplitude c_{Fl} in the asymptotic limit $\delta l \to \infty$, as long as they are not attractive enough to bind the membranes; exactly at the critical strength of these interactions, c_{Fl} is decreased by a factor of 12 [7].

Figure 1*b*) gives the ratio of the separation in a symmetric stack of three membranes (averaged over the two difference coordinates) and a stack of two membranes. This ratio reaches unity for $p \lesssim 10^{-2}$ within the numerical error, which is the pressure range for which the data scale accurately, see fig. 1*a*). In fig. 1*c*) we include data for a symmetric stack of four membranes, where we have to differentiate between the inner separation $\langle \delta z_{\mathrm{I}} \rangle \equiv \langle \delta z_2 \rangle$ and the outer separation $\langle \delta z_{\mathrm{O}} \rangle \equiv \langle \delta z_1 + \delta z_3 \rangle / 2$. The ratio between the separation for $N = 3$ and the outer separation for $N = 4$ is close to unity already for rather high pressures; the ratio of the inner and the outer separations for $N = 4$ approaches unity within the numerical error for $p \lesssim 10^{-2}$, as in fig. 1*b*). It is clear from the data that the estimate of c_{Fl} for $N = 3$ and 4 agrees with the value obtained for $N = 2$ within the numerical accuracy; there is a small trend to a lower c_{Fl} as N increases (open circles in fig. 1*b*) and *c*)), which is, however, exceeded by the numerical error for $p \lesssim 10^{-2}$. Thus, based on the accessible range of length scales and the limited number of membranes considered, the asymptotic form of the fluctuation repulsion does not depend on the number of membranes, and the relative displacement fields in a stack decouple for small pressure [3].

This result can be further substantiated by considering asymmetric stacks. In fig. 2*a*) we show data for a stack of two membranes on a flat substrate. Again, all lengths scale

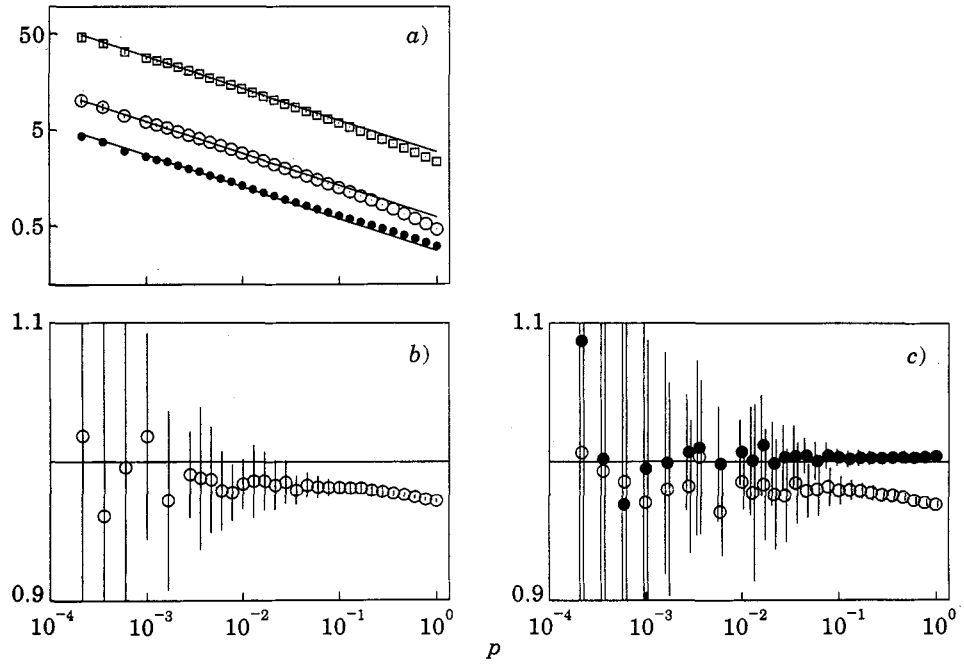

Fig. 1. – MC results for tensionless, symmetric stacks as a function of rescaled pressure p; vertical lines denote numerical errors. *a*) Mean separation $\langle \delta z \rangle$ (○), roughness $\langle \delta z^2 \rangle_c^{1/2}$ (●), and parallel correlation length $\xi_{\parallel}$ (□) for two membranes, $N = 2$. *b*) Ratio of mean separations for stacks of three and two membranes. *c*) Ratio of the mean separations of three membranes and the outer separations $\langle \delta z_{\mathrm{O}} \rangle$ of four membranes (●) and ratio of the inner and outer separations $\langle \delta z_{\mathrm{I}} \rangle$ and $\langle \delta z_{\mathrm{O}} \rangle$ in a stack of four membranes (○).

[3] The independence of the displacement fields in a stack, or the quasi-separability, breaks down if one chooses the pressure between the pairs of membranes to be different, as appropriate for quaternary systems, where consecutive spacings between the amphiphilic sheets can be different.

asymptotically as $\sim p^{-1/3}$. The ratios of the two displacement fields are given in fig. 2*b*) for the separations and the parallel correlation lengths, which approach $2^{1/3}$ and $2^{-1/6}$, respectively, as denoted by the broken lines. Treating the two membrane pairs as independent, it follows that the relative displacement field of the membrane/flat substrate pair is governed by a bending modulus which is twice as large as that for the relative displacement field of two identical membranes. Using the above-given scaling forms for ℓ and $\xi_\parallel$, one obtains the ratios $2^{1/3}$ and $2^{-1/6}$. In fig. 2*c*) the results for the asymmetric system of three membranes on a flat substrate are shown; here we average over the two displacement fields between the upper three membranes, since they turn out to be equivalent (within the numerical error). The remaining two sets of data show the same behavior as the data in fig. 2*a*). For asymmetric stacks, the different displacement fields again decouple and are each described by a fluctuation amplitude c_{FI} which agrees with the estimate for symmetric stacks. This behavior is very different from that of stacks of membranes which are bound by short-ranged attractive forces between the membranes; in the latter case, a flat substrate affects the whole stack and leads to a sequence of unbinding transitions [5].

For the investigation of the effects of non-vanishing lateral tension σ, it should thus be sufficient to treat a single symmetric pair of membranes. The scaling of the fluctuation repulsion can be obtained by considering one hump of the relative displacement field (which is governed by the effective rigidity $\bar{\kappa} = \kappa/2$ and the effective tension $\bar{\sigma} = \sigma/2$) with linear size $\xi_\parallel$ and replacing the confining potential by the low-momentum cut-off $q_{\min} = c_{\min}/\xi_\parallel$. The

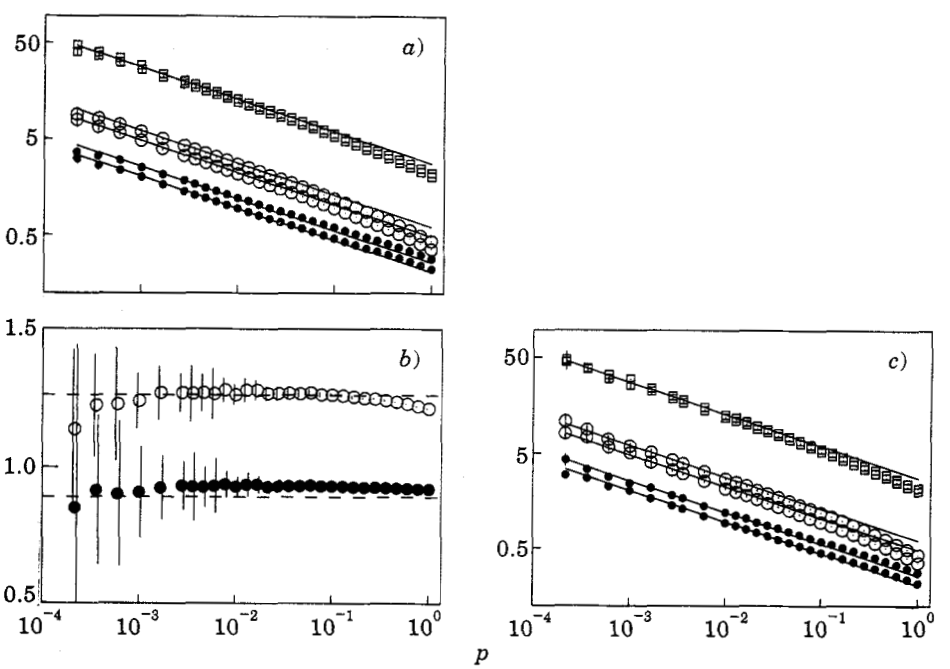

Fig. 2. – MC results for tensionless, asymmetric stacks. *a*) Separate data for the upper and the lower displacement fields in a stack of two membranes on a flat substrate; the symbols have the same meaning as in fig. 1*a*). *b*) Same data now plotted as ratios of the two distinct displacement fields for the separations $\langle \delta z \rangle$ (○) and the parallel correlation lengths $\xi_\parallel$ (●). *c*) Data for a stack of three membranes on a flat substrate; the two sets of data correspond to the lowest displacement field adjacent to the substrate and an average over the upper two displacement fields; the symbols have the same meaning as in fig. 1*a*).

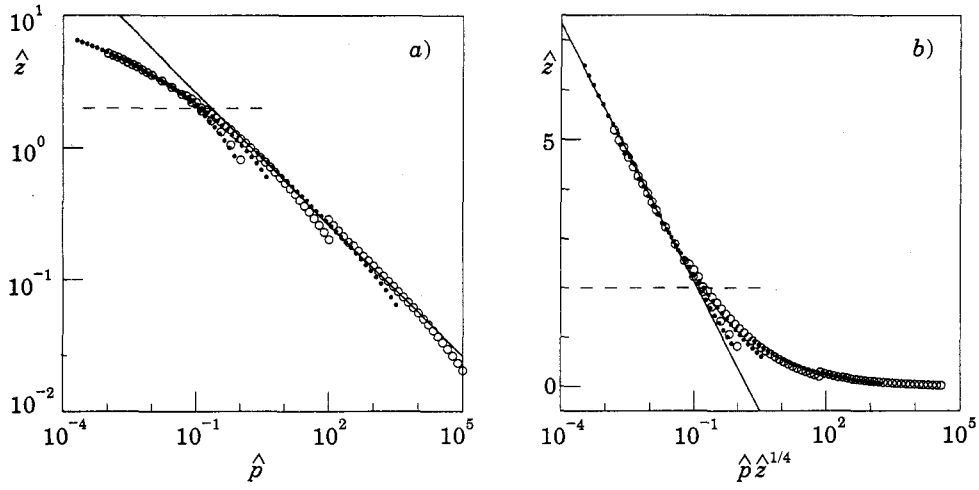

Fig. 3. – Scaling plots for six sets of data carried out at different values of $\omega \sim \sqrt{\sigma/\kappa}$; the data points on the left and on the right correspond to large and to small values of ω, respectively. *a*) The straight line denotes $\hat{z} \sim \hat{p}^{-1/3}$, as realized in the bending-dominated regime. *b*) The straight line denotes $\hat{z} \sim \ln(\hat{p}\hat{z}^{1/4})$, as observed in the tension-dominated regime.

corresponding roughness $\xi_\perp$ is then given by

$$\xi_\perp^2 = T \int' \frac{\mathrm{d}^2 q}{(2\pi)^2} \frac{1}{\bar{\sigma} q^2 + \bar{\kappa} q^4} = (l_\sigma^2/2) \ln \left[\frac{1 + (\xi_\parallel \omega / c_{\min} a_\parallel)^2}{1 + (\omega/c_{\max})^2} \right], \tag{3}$$

with the crossover length $l_\sigma \equiv \sqrt{T/2\pi\bar{\sigma}}$. The prime at the integral indicates that the integration is restricted to $q_{\min} < q < q_{\max}$, where the high-momentum cut-off is $q_{\max} = c_{\max}/a_\parallel$. Using $V_{\mathrm{Fl}} \approx bT/\xi_\parallel^2$, which is a representation of the equipartition theorem, and inverting (3), one obtains V_{Fl} as a function of $\xi_\perp$.

For large ω, the fluctuations are dominated by the lateral tension on all scales. In this case, the roughness and the mean separation satisfy the scaling relation $2(\xi_\perp/l_\sigma)^2 \approx \ell/l_\sigma + \ln(\ell/l_\sigma)/4$ [12], and the fluctuation-induced interaction behaves as

$$V_{\mathrm{Fl}}(\ell) \approx (b_0 T/a_\parallel^2) \exp[-\ell/l_\sigma](l_\sigma/\ell)^{1/4}, \tag{4}$$

with the parameter-independent coefficient $b_0 \sim b(c_{\max}/c_{\min})^2$ (note that the same behavior is found for complete wetting in three dimensions).

For small ω, one must distinguish a rigidity-dominated regime with $\xi_\perp \ll l_\sigma$, and a tension-dominated regime with $\xi_\perp \gg l_\sigma$ [1]. In the rigidity-dominated regime, one has the scaling relation $\ell \approx \mathcal{G}_\perp \xi_\perp$, and the fluctuation-induced interaction $V_{\mathrm{Fl}}(\xi_\perp)$ reduces to the form as given by (1) with $c_{\mathrm{Fl}}/2 = b\mathcal{G}_\perp^2/4\pi c_{\min}^2$. In the tension-dominated regime, one recovers the functional form as in (4) but with the prefactor $b_0 T/a_\parallel^2$ replaced by $(b_0/c_{\max}^2) T\sigma/\kappa$.

The general scaling form of $V_{\mathrm{Fl}}(\ell)$, which contains both (1) and (4) as limiting cases, can be written as

$$V_{\mathrm{Fl}}(\ell) \equiv \frac{\omega^2/a_\parallel^2}{c_{\max}^2 + \omega^2} T\Phi(\ell\sqrt{\sigma/T}), \tag{5}$$

which yields, after minimization of the expression $V_{\mathrm{Fl}}(\ell) + P\ell$, the scaling form for the separation

$$\Phi'(\tilde{z}) \equiv \Phi'(\delta z \omega) = -p(c_{\max}^2 + \omega^2)/\omega^3 \equiv -\tilde{p}, \tag{6}$$

where the prime denotes a derivative with respect to $\hat{z}$, and $\hat{z}$ and $\hat{p}$ are rescaled separation and pressure variables.

We carried out six different simulation series for the model as given by (1) with $N = 2$ and $\omega^2 = 0.002, 0.02, \ldots, 200$. Figure 3*a*) shows a double-log scaling plot of $\hat{z}$ as a function of $\hat{p}$, where the expected behavior in the rigidity-dominated regime, $\hat{p} \sim \hat{z}^{-3}$ from (1), is denoted by a straight line. For the dimensionless coefficient $c_{\max}$ we obtain the estimate $c_{\max} = 3.0 \pm 0.1$ leading to $b_0 \simeq 1.3$, which determines the amplitude of the fluctuation-induced repulsion V_{Fl} in the tension-dominated regime. For mean spacings larger than a crossover value, lateral tension strongly reduces the strength of V_{Fl} as compared to the tension-free case and changes the functional dependence of the spacing on the pressure. In fig. 3*b*) the same data are shown in a different plot with the expected behavior for the tension-dominated regime, $\ln(\hat{p}) \sim \hat{z} - \ln(\hat{z})/4$ from (4), again denoted by a straight line. In each of the regimes, the data are accurately described by the asymptotic forms of the fluctuation potential as given by (1) and (4); the crossover length is given by $\hat{z}^* \simeq 2$, which is denoted by broken lines, the corresponding crossover pressure is $\hat{p}^* \simeq 0.1$. Typical lateral tensions in multilamellar structures range from $\sigma \simeq 10^{-9}$ to $10^{-6}\,\mathrm{J/m^2}$ [3], and are strictly bounded above by the tension of rupture, which is $\simeq 10^{-3}\,\mathrm{J/m^2}$. The characteristic membrane spacing at which the system crosses over from the rigidity-dominated regime, at small spacings, to the tension-dominated regime, at large separations, is thus given by $l^* = \hat{z}^* \sqrt{T/\sigma} \simeq 2$–$2000\,\mathrm{nm}$ at room temperatures, which does not depend on the pressure or the bending modulus and lies within the range of observable layer spacings [2, 8]. Even the effect of a small lateral tension should therefore be experimentally observable for large separations. The crossover pressure is given by $P^* \simeq (\hat{p}^*/c_{\max}^2)\sqrt{\sigma^3 T/\kappa^2} \simeq 10^{-7}$–$10^2\,\mathrm{J/m^3}$, where $\kappa \simeq 10^{-19}\,\mathrm{J}$ for lipid bilayers has been used. In an experiment where the layer spacing is not fixed, such low pressures can be produced by osmotic stress techniques, which cover the pressure range of up to $10^6\,\mathrm{J/m^3}$ [2].

REFERENCES

[1] For recent reviews, see LIPOWSKY R., *J. Phys. Condens. Matter A*, **6** (1994) 405, and *The Structure and Dynamics of Membranes*, edited by R. LIPOWSKY and E. SACKMANN, *Handbook on Biological Physics*, Vol. 1 (Elsevier, Amsterdam) in press.

[2] See, *e.g.*, PARSEGIAN V. A., FULLER N. and RAND R. P., *Proc. Natl. Acad. Sci. USA*, **76** (1979) 2750; RAND R. P. and PARSEGIAN V. A., *Biochim. Biophys. Acta*, **988** (1989) 351.

[3] SERVUSS R. M. and HELFRICH W., *J. Phys. (Paris)*, **50** (1989) 809; HARBICH W. and HELFRICH W., *J. Phys. (Paris)*, **51** (1990) 1027; MUTZ M., SERVUSS R.-M. and HELFRICH W., *J. Phys. (Paris)*, **51** (1990) 2557.

[4] HELFRICH W., *Z. Naturforsch.*, **33a** (1978) 305; HELFRICH W. and SERVUSS R.-M., *Nuovo Cimento D*, **3** (1984) 137.

[5] NETZ R. R. and LIPOWSKY R., *Phys. Rev. Lett.*, **71** (1993) 3596.

[6] LIPOWSKY R. and ZIELINSKA B., *Phys. Rev. Lett.*, **62** (1989) 1572.

[7] NETZ R. R., to be published in *Phys. Rev. E*.

[8] ROUX D. and SAFINYA C. R., *J. Phys. (Paris)*, **49** (1988) 307.

[9] DAVID F., *J. Phys. (Paris)*, **51** (1990) C7-115.

[10] GOMPPER G. and KROLL D. M., *Europhys. Lett.*, **9** (1989) 59.

[11] JANKE W., KLEINERT H. and MEINHART M., *Phys. Lett. B*, **217** (1989) 525.

[12] LIPOWSKY R. AND GROTEHANS S., *Europhys. Lett.*, **23** (1993) 599; *Biophys. Chem.*, **49** (1994) 27.